Supplementary material for the publication:

Gas-to-particle partitioning of major biogenic oxidation products from monoterpenes and real plant emissions

Table S1: Major compounds identified as parent ions from the PTR-based techniques that have been observed in previous publications. Suggested names and structures are attributed to the chemical formula that was identified by the PTR-based techniques.

	Chemical formula	MW	Structure	SMILES code
β-pinene (Chen and Griffin, 2005; Hohaus et al., 2015; Jenkin, 2004; Yu et al., 1999)				
Nopinone	$C_9H_{14}O$	138.21	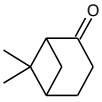	CC1(C2CC1C(=O)CC2)C
2,2-Dimethyl-cyclobutane-1,3-dicarboxaldehyde	$C_8H_{12}O_2$	140.18	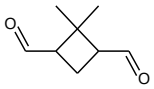	O=CC1CC(C=O)C1(C)C
Oxonopinone	$C_9H_{12}O_2$	152.19	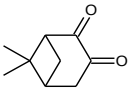	CC1(C2CC1C(=O)C(=O)C2)C
2,2-Dimethyl-3-formyl-cyclobutyl-methanoic acid	$C_8H_{12}O_3$	156.18	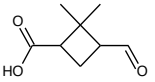	OC(=O)C1CC(C=O)C1(C)C
Norpinonic acid top/ Pinalic-3-acid middle/ Pinalic-4-acid bottom	$C_9H_{14}O_3$	170.21	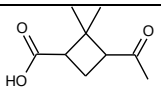	OC(=O)C1CC(C(C)=O)C1(C)C
			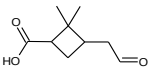	OC(=O)C1CC(CC=O)C1(C)C
			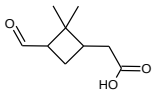	OC(=O)CC1CC(C=O)C1(C)C
Norpinic acid	$C_8H_{12}O_4$	172.18	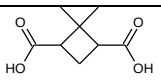	CC1(C(CC1C(=O)O)C(=O)O)C
Hydroxy norpinonic acids	$C_9H_{14}O_4$	186.21	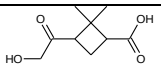	OC(=O)C1CC(C(=O)CO)C1(C)C
			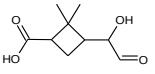	OC(C=O)C1CC(C(=O)O)C1(C)C

Pinic acid	$C_9H_{14}O_4$	186.21	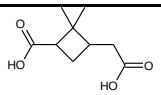	CC1(C(CC1C(=O)O)CC(=O)O)C

Limonene **(Chen and Griffin, 2005; Jaoui et al., 2006; Kundu et al., 2012; Leungsakul et al., 2005a; Leungsakul et al., 2005b)**				
3,6-Oxoheptanoic acid	$C_7H_{10}O_4$	158.15	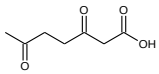	O=C(CCC(C)=O)CC(=O)O
			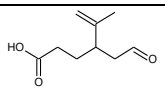	O=CCC(CCC(=O)O)C(=C)C
Limonalic acid/ Norlimononic acid/ Ketolimononaldehyde	$C_9H_{14}O_3$	170.21	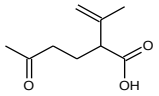	O=C(C)CCC(C(=C)C)C(=O)O
			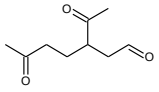	CC(=O)C(CC=O)CCC(=O)C
			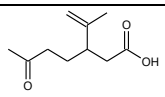	O=C(C)CCC(CC(=O)O)C(=C)C
Limononic acid/ 4-Isopropenyl-1-methyl-1,5-hydroxy-2-oxocyclohexane/ 7-Hydroxylimononaldehyde	$C_{10}H_{16}O_3$	184.23	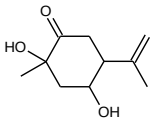	CC(=C)C1CC(=O)C(C)(O)CC1O
			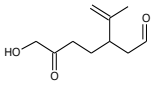	O=C(CCC(CC=O)C(=C)C)CO
Ketolimononic acid/ Limonic acid	$C_9H_{14}O_4$	186.21	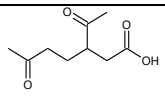	O=C(C)CCC(CC(=O)O)C(C)=O
			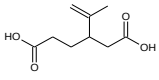	OC(=O)CCC(CC(=O)O)C(=C)C
5-Hydroxylimononic acid/ 7-Hydroxylimononic acid	$C_{10}H_{16}O_4$	200.23	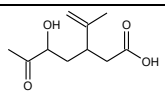	O=C(C)C(O)CC(CC(O)=O)C(=C)C
			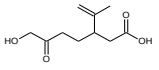	O=C(CCC(CC(=O)O)C(=C)C)CO

Trees (α-pinene / Δ^3-carene) **(Chen and Griffin, 2005; Praplan et al., 2014; Yu et al., 1999)**				
3-Norcaronic acid and isomers	$C_9H_{14}O_3$	170.21	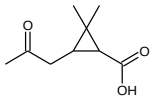	O=C(C)CC1C(C(=O)O)C1(C)C
				OC(=O)CC1C(CC=O)C1(C)C
			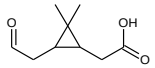	OC(=O)CC1C(CC=O)C1(C)C
Norpinic acid / Nor-3-caric acid	$C_8H_{12}O_4$	172.18	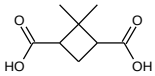	CC1(C(CC1C(=O)O)C(=O)O)C
2,2-Dimethyl-3-formyl-cyclobutyl-methanoic-acid/ Pinonic acid / 3-caronic acid/ Hydroxy pinonaldehydes	$C_{10}H_{16}O_3$	184.23	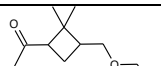	O=C(C)C1CC(COC=O)C1(C)C
			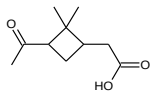	OC(=O)CC1CC(C(C)=O)C1(C)C
			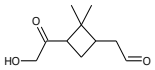	O=C(CO)C1CC(CC=O)C1(C)C
			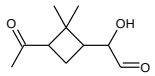	OC(C=O)C1CC(C(C)=O)C1(C)C
Pinic acid / 3-Caric acid	$C_9H_{14}O_4$	186.21	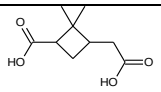	CC1(C(CC1C(=O)O)CC(=O)O)C

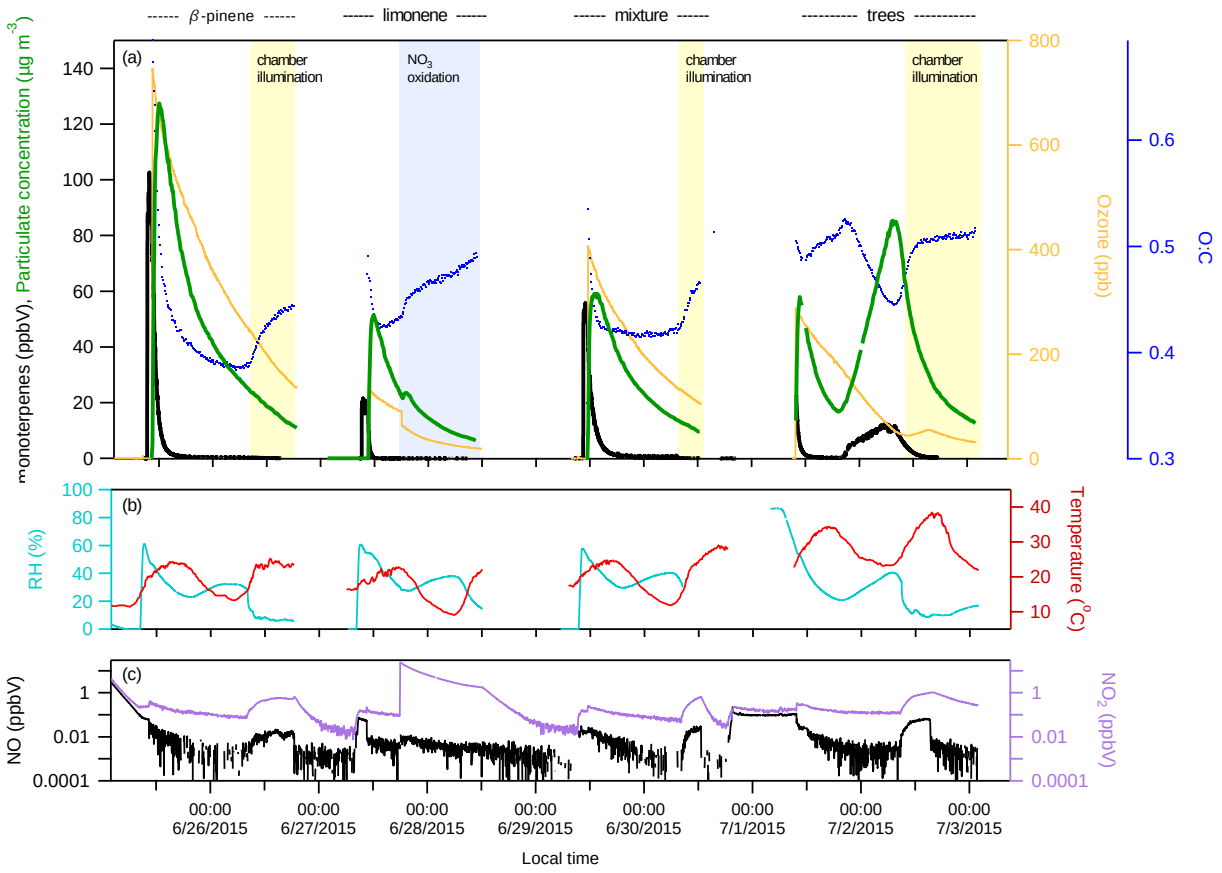

Figure S1: An overview of all experiments during the campaign with (a) corresponding to the mixing ratios of the injected monoterpenes (black line) and ozone (orange line) as well as the SOA mass produced (green line) and its O:C ratio as an indicator of the oxidation of the SOA. Background colours correspond to the opening of the roof (yellow) or the NO_3 oxidation initiation (blue colour). Measurement of the RH (ciel), temperature (red), NO (black) and NO_2 (purple) are also provided.

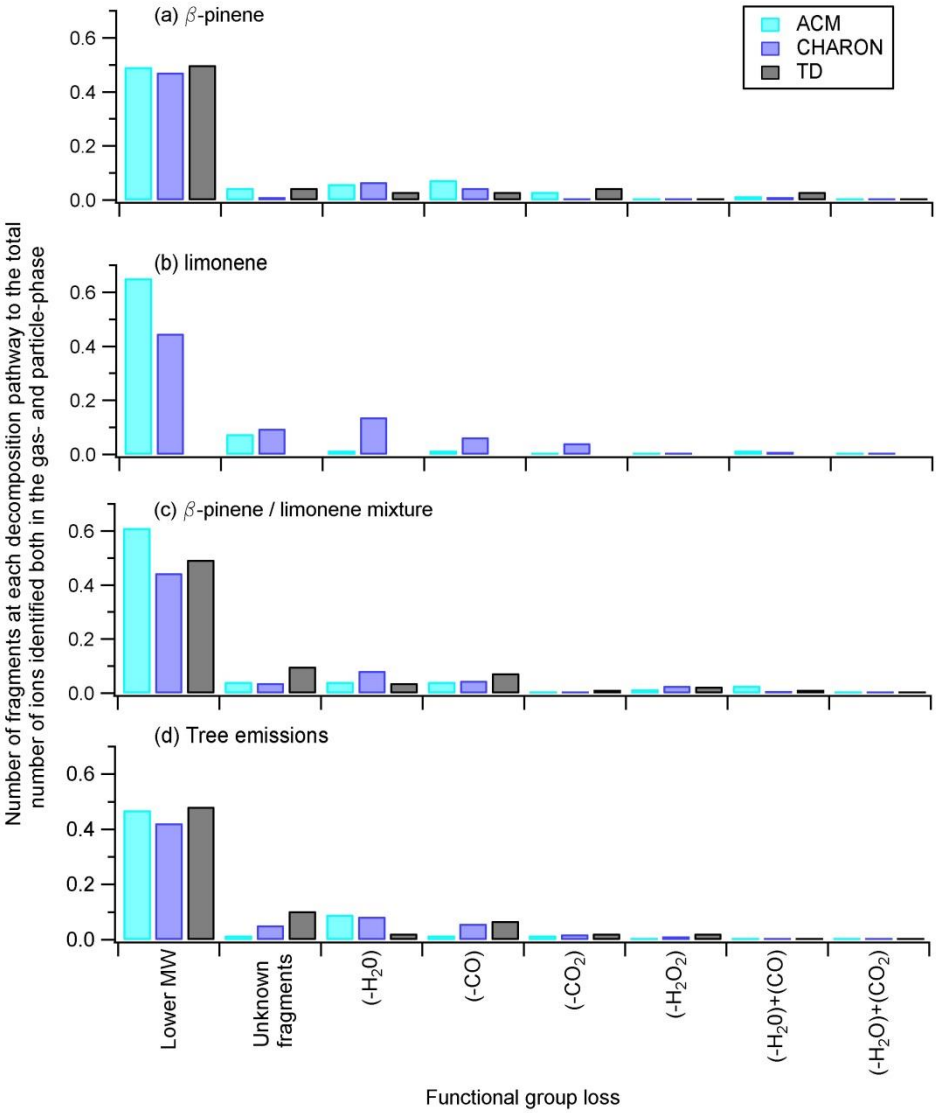

Figure S2: The ratio of the number of lower molecular weight and unknown fragments as well as fragments subject to functional group loss ((-H_2O), (-CO) (-CO_2), (-H_2O_2), (-H_2O) and (-CO), (-H_2O) and (-CO_2)) to the number of identified ions both in the gas- and particle-phase. Different colours indicate the different instruments for the different experiments.

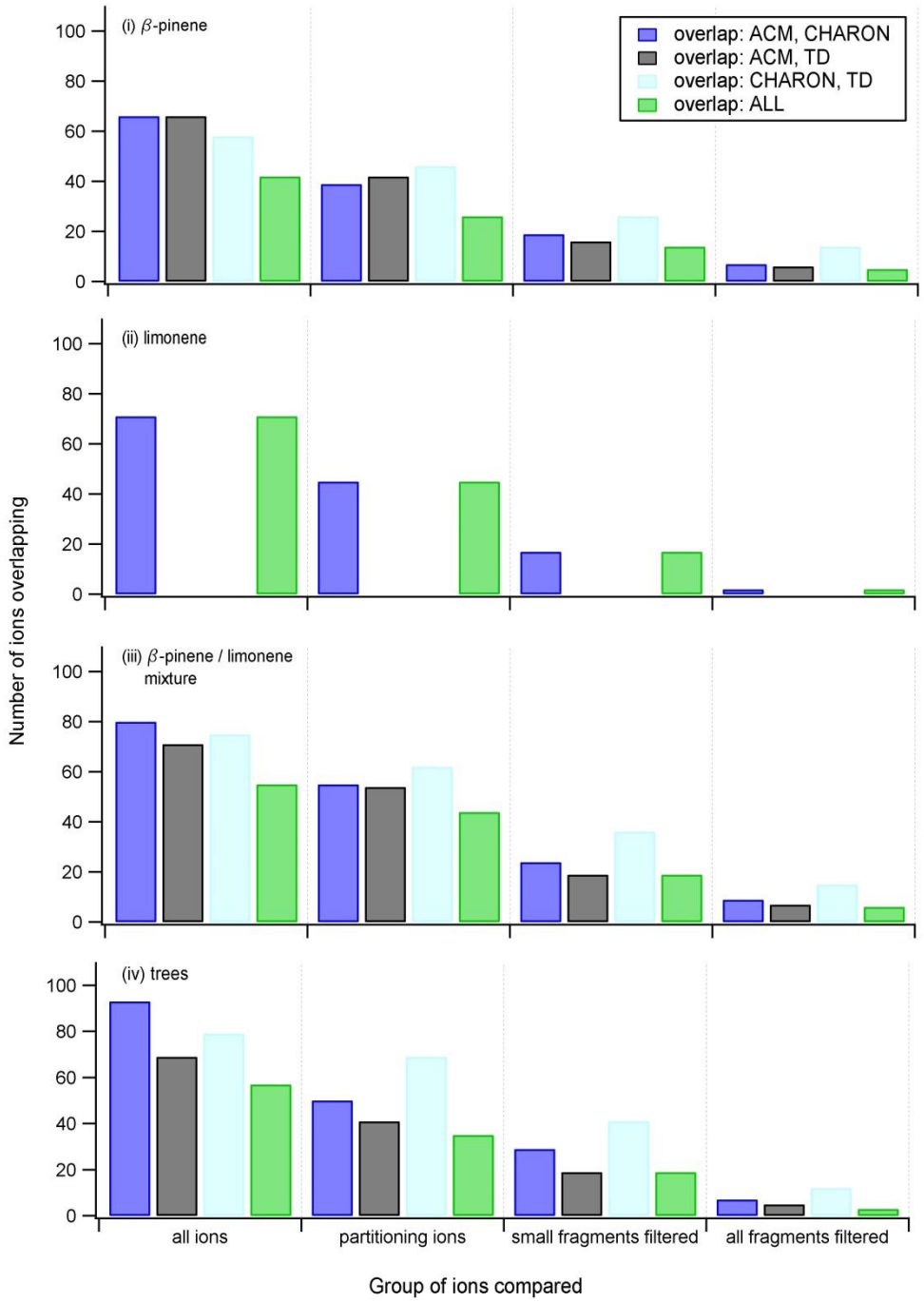

Figure S3: The number of ions measured from more than one technique with a focus on the ions measured both from ACM and CHARON (blue), ACM and TD (black), CHARON and TD (ciel) and ions measured from all techniques, accounting for ACM, TD and CHARON (green). Overlaps are checked for different groups of ions starting from the overlaps of all ions detected, to overlaps seen for only the ions that partition between the gas- and particle-phase, to the overlaps of the remaining partitioning ions after filtering out the small fragments and the remaining partitioning ions after filtering out all fragments for the different experiments performed.

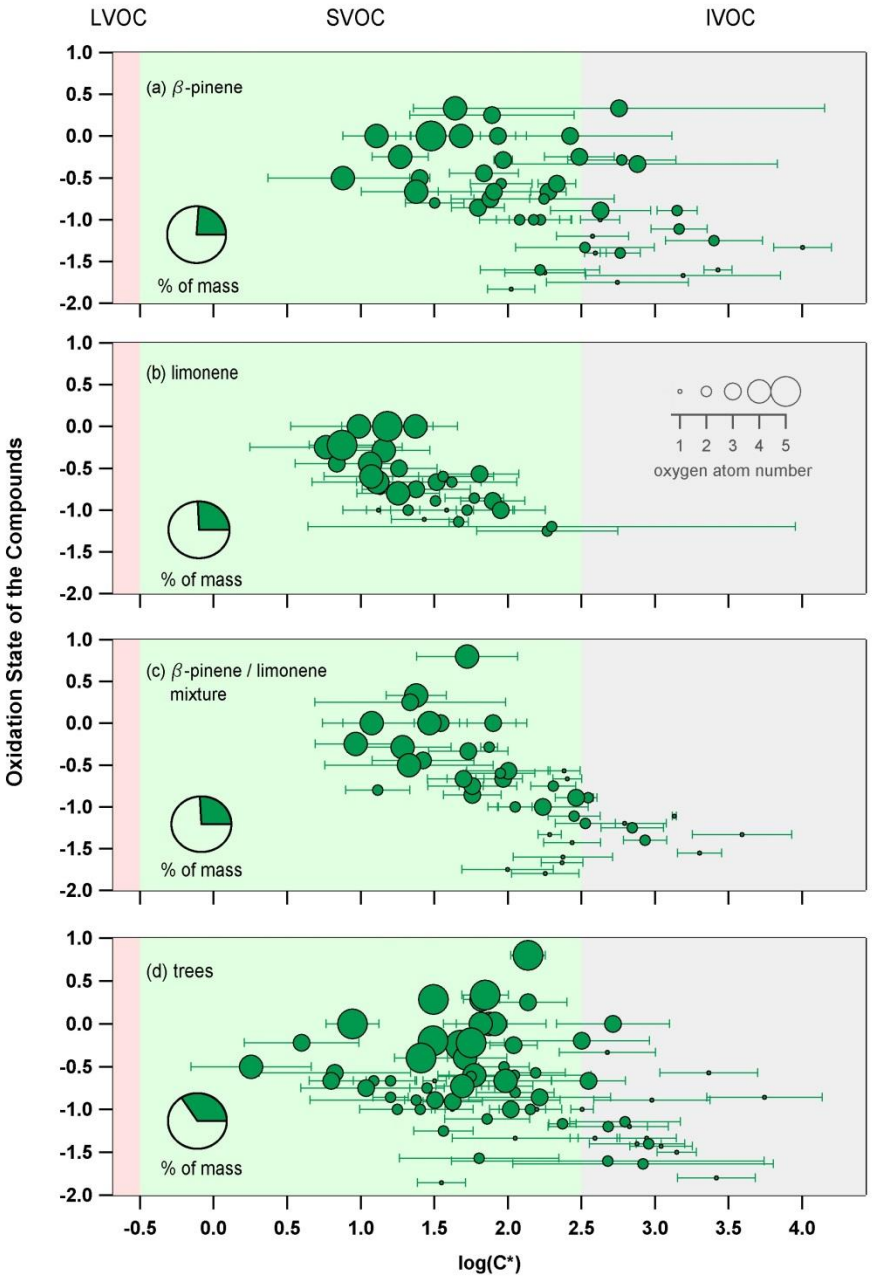

Figure S4: The average experimental saturation concentration for detected ions (from ACM and CHARON) that act as parent ions identified using the described selection criteria during the different experiments. Error bars indicate the ± 1σ of the average. Size of the markers is an indicator of the oxygen atom number for each species. Pie charts show the percent of mass (green) measured when adding all presented ions compared to the total organic mass obtained from the AMS.

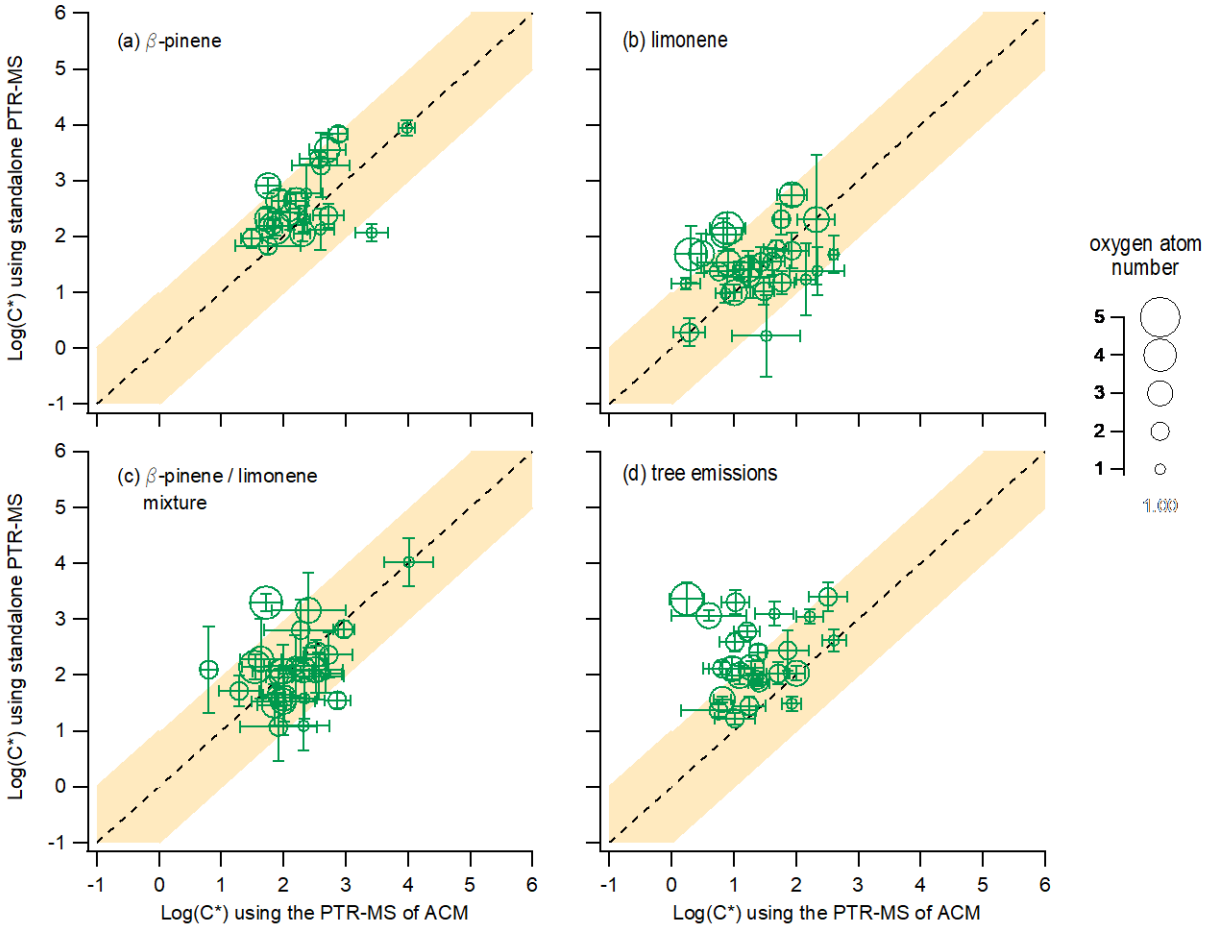

Figure S5: The average saturation mass concentration from the individual experiments for the ACM when using the gas-phase mass concentration values obtained from the PTR-MS of ACM (x-axis) in comparison to the standalone PTR-MS (y-axis). Error bars indicate the ± 1σ of the average. Size of the markers is an indicator of the oxygen atom number for each species.

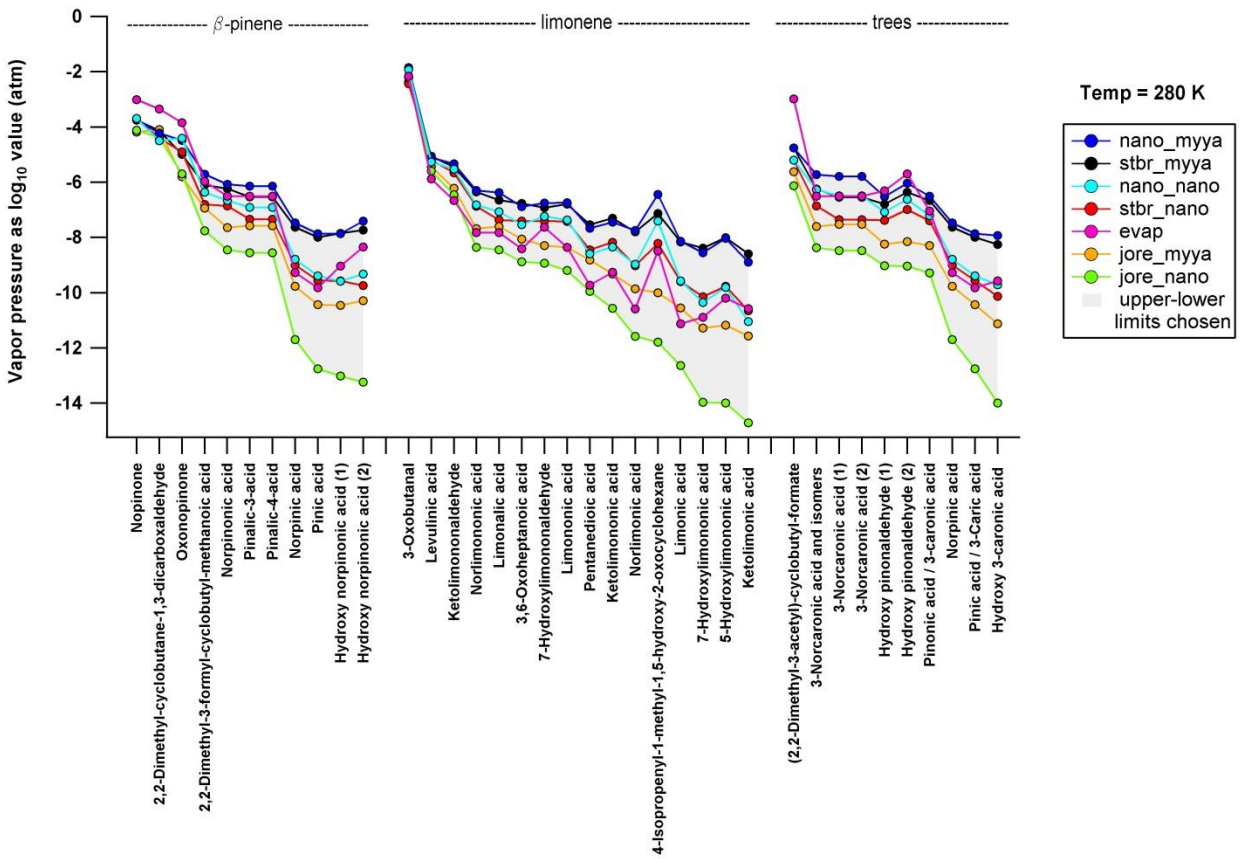

Figure S6: Theoretical calculation of the vapor pressure (y-axis) using the combination of 7 different approaches. The grey background color indicates the minimum and maximum range chosen for this study. Details on the different approaches are provided in section 2.4.

References

Chen, J., and R. Griffin: Modeling secondary organic aerosol formation from oxidation of -pinene, -pinene, and -limonene, *Atmospheric Environ.*, *39*(40), 7731-7744, doi:10.1016/j.atmosenv.2005.05.049, 2005.

Hohaus, T., I. Gensch, J. R. Kimmel, D. R. Worsnop, and A. Kiendler-Scharr: Experimental determination of the partitioning coefficient of β-pinene oxidation products in SOAs, *Phys. Chem. Chem. Phys.*, *17*(22), 14796-14804, doi:10.1039/C5CP01608H, 2015.

Jaoui, M., E. Corse, T. E. Kleindienst, J. H. Offenberg, M. Lewandowski, and E. O. Edney: Analysis of secondary organic aerosol compounds from the photooxidation of d-limonene in the presence of NOX and their detection in ambient PM2.5, *Environ Sci Technol*, *40*(12), 3819-3828, doi:10.1021/es052566z, 2006.

Jenkin, M. E.: Modelling the formation and composition of secondary organic aerosol from α- and β-pinene ozonolysis using MCM v3 *Atmos. Chem. Phys.*, *4*, 1741-1757, 2004.

Kundu, S., R. Fisseha, A. L. Putman, T. A. Rahn, and L. R. Mazzoleni: High molecular weight SOA formation during limonene ozonolysis: insights from ultrahigh-resolution FT-ICR mass spectrometry characterization, *Atmos. Chem. Phys.*, *12*(12), 5523-5536, doi:10.5194/acp-12-5523-2012, 2012.

Leungsakul, S., M. Jaoui, and R. M. Kamens: Kinetic mechanism for predicting secondary organic aerosol formation from the reaction of d-limonene with ozone, *Environ Sci Technol*, *39*(24), 9583-9594, doi:10.1021/es0492687, 2005a.

Leungsakul, S., H. E. Jeffries, and R. M. Kamens: A kinetic mechanism for predicting secondary aerosol formation from the reactions of d-limonene in the presence of oxides of nitrogen and natural sunlight, *Atmospheric Environ.*, *39*(37), 7063-7082, doi:10.1016/j.atmosenv.2005.08.024, 2005b.

Praplan, A. P., S. Schobesberger, F. Bianchi, M. P. Rissanen, M. Ehn, T. Jokinen, H. Junninen, A. Adamov, A. Amorim, J. Dommen, et al.: Elemental composition and clustering of α-pinene oxidation products for different oxidation conditions, *Atmos. Chem. Phys. Discuss.*, *14*(22), 30799-30833, doi:10.5194/acpd-14-30799-2014, 2014.

Yu, J., D. R. Cocker, R. J. Griffin, R. C. Flagan, and J. H. Seinfeld: Gas-phase ozone oxidation of monoterpenes: Gaseous and particulate products, *J. Atmos. Chem.*, *34*(2), 207-258, doi:10.1023/a:1006254930583, 1999.